# 7.0 TEPHROCHRONOLOGIC STUDIES

Compiled by Craig E. Skinner*
with contributions by Kurt T. Katsura*

## 7.1 INTRODUCTION

During the course of the PGT-PG&E Pipeline Expansion Project (PEP) 60 samples of volcanic tephra from 21 archaeological sites were selected for tephrochronologic investigation and geochemical characterization (Figure 7-1 and Table 7-1). Sample provenance and geochemical data for all analyzed tephra samples are presented in Tables 7-2 and 7-3. Thirty-three samples were analyzed during the first phase of the Project; letter reports by Dr. Franklin F. Foit, Washington State University, describing the results of electron microprobe analysis of these samples are included in Lebow et al. (1991). Letter reports describing the subsequent analyses of additional tephra samples recovered during 1991–1992 testing and data recovery efforts are presented in Speulda et al. (1992). The remaining letter reports by Dr. Foit describing tephra analyses conducted during 1992 and 1993 appear at the end of this chapter. The following discussion of volcanic tephra is comprehensive and covers all 60 samples analyzed as part of the Project.

## 7.2 GEOLOGIC SOURCES OF VOLCANIC TEPHRA IN THE PROJECT AREA

### 7.2.1 Introduction

The term volcanic tephra refers to ejecta or fragmental material that is blown through the air by explosive volcanic eruptions (Williams and McBirney 1979). Most of the tephra consists of molten rock that is blown into the air and quenched, forming fragmental glass shards that are carried away from the vent by dense debris-flow clouds (ignimbrites) or by the wind. The airborne pyroclastic ejecta and the deposits which they form are commonly classified and referred to according to the following particle-size groups proposed by Fisher (1961): blocks and bombs (>64 mm), lapilli (2.0-64 mm), and ash (<2.0 mm). The term *tephra* is used here to describe all airfall fragmental volcanic material regardless of sorting or particle-size; specific particle-size terms are used to denote the individual fragments and the deposits which they form. For example, ash beds refer to a deposits of ash-size particles that form a definable sedimentary unit.

Airfall deposits of volcanic ash can occur hundreds of kilometers downwind from their parent vents, while ash-flow deposits (ignimbrites) are usually limited in distance to a few tens of kilometers (Fisher and Schmincke 1984). Many of the widely distributed rhyolitic airfall tephra deposits found throughout the western United States, including parts of the central and northern Project area, have been correlated using geochemical data from known sources of tephra eruptions. When these tephra sources and deposits are well dated, as with the

---
* INFOTEC Research, Inc.

Holocene eruptions in Washington, Oregon, and California, the use of tephrochronologic methods can add an important temporal component to archaeological studies in the Far West.

While there is no doubt that volcanic ash falls had an effect on prehistoric populations inhabiting the Project area, the specific outcomes and magnitude of impact are not known. Ethnographic accounts of ash falls from Mount St. Helens, Washington, for example, suggest that short-term effects of volcanic ash falls may catastrophically disrupt annual subsistence cycles (Ray 1932; Teit 1930). As research following the 1980 eruptions of Mount St. Helens showed, however, even severe damage to vegetation and faunal resources is likely to be ephemeral and the long-term impact is likely to be minimal (Matz 1991:9–25).

Table 7-1 Summary of All Samples of Volcanic Tephra Selected for Tephrochronologic Investigation During Testing and Data Recovery Phases of the Project.

| Site | Number of Samples | Number of Sources [a] | Mazama? | John Day Formation [b] |
|---|---|---|---|---|
| CA-MOD-2561 | 1 | 1 | No | No |
| CA-MOD-2573 | 1 | 2 | Yes | No |
| 10-BY-309 | 2 | 1 | Yes | No |
| 35-DS-263 | 1 | 1 | No | No |
| 35-DS-557 | 1 | 2 | No | No |
| 35-GM-25 | 2 | 1 | Yes | No |
| 35-GM-103 | 1 | 1 | No | No |
| 35-JE-49 | 8 | 9 | Yes | Yes |
| 35-JE-50 | 2 | 2 | Yes | Yes |
| 35-JE-51B | 11 | 3 | Yes | Yes |
| 35-JE-283 | 4 | 4 | Yes | Yes |
| 35-JE-288 | 1 | 2 | Yes | Yes |
| 35-JE-289 | 1 | 1 | Yes | No |
| 35-JE-296 | 1 | 1 | Yes | No |
| 35-JE-298 | 1 | 1 | Yes | No |
| 35-SH-134 | 3 | 1 | Yes | No |
| 35-UM-154 | 3 | 3 | Yes | No |
| 35-WS-120 | 3 | 6 | Yes | No |
| 35-WS-223 | 1 | 2 | Yes | Yes |
| 35-WS-225 | 4 | 1 | Yes | No |
| 35-WS-226 | 1 | 1 | Yes | No |
| 35-WS-231 | 3 | 1 | Yes | No |
| 35-WS-232 | 1 | 1 | Yes | No |
| 35-WW-100 | 2 | 2 | Yes | No |
| 35-WW-101 | 1 | 1 | Yes | No |

[a] Number of potentially distinguishable geochemical groups of volcanic tephra sources identified at the site.
[b] If yes, then John Day Formation tephra was identified at the site.

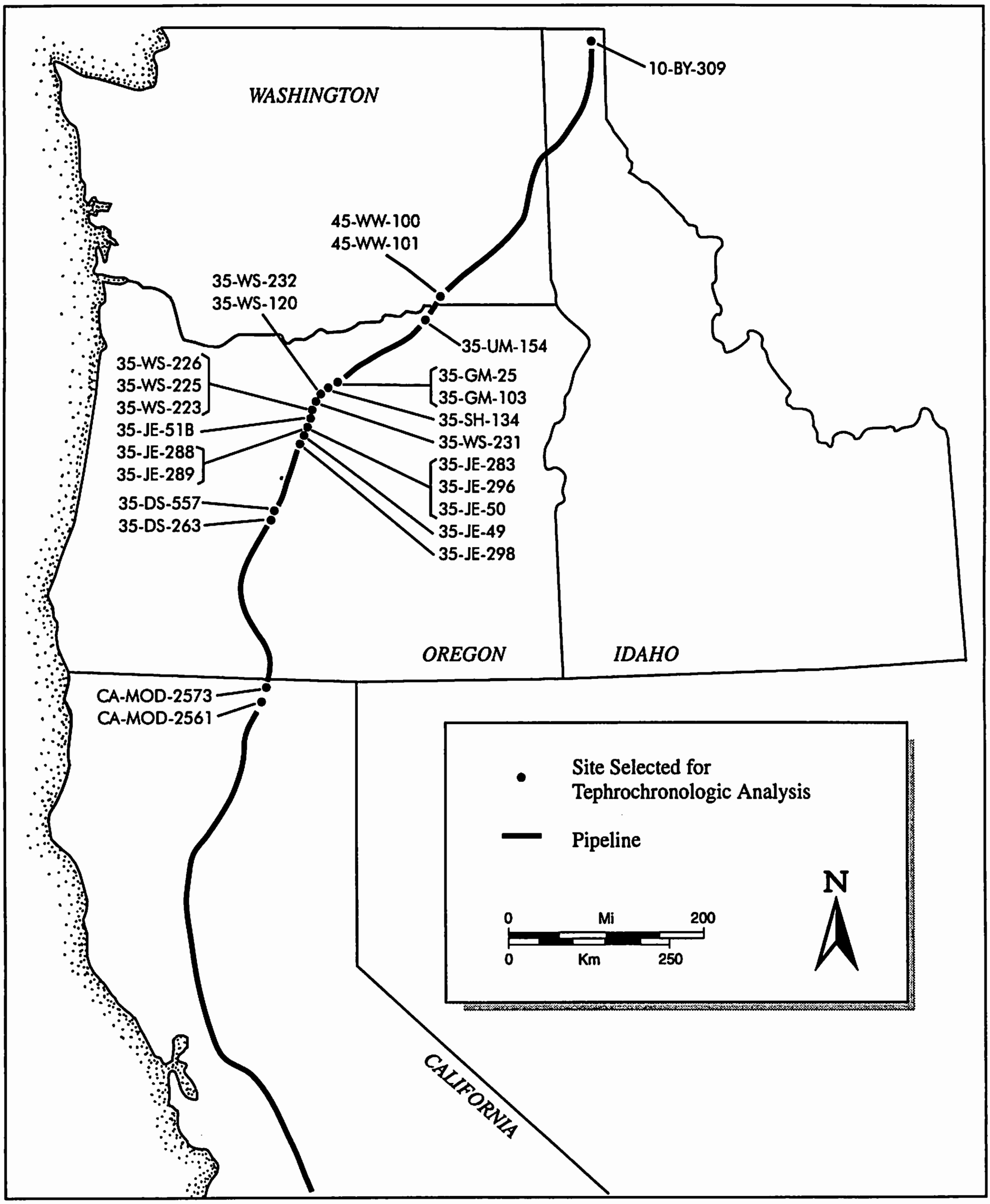


Figure 7-1 Location of all PEP Sites in Idaho, Washington, Oregon, and California yielding samples selected for tephrochonologic investigation.

### 7.2.2 Potential Sources of Volcanic Ash

Many different tephra deposits of Holocene and Pleistocene age have been identified in the regions crossed by the Project (see Figure 7-2). Overview studies of many of these sources and their resultant deposits are found in Sarna-Wojcicki and Davis (1991), Sarna-Wojcicki et al. (1983, 1991), and Skinner and Radosevich (1991).

**Glacier Peak, Washington.** Multiple late Pleistocene eruptions of volcanic ash at Glacier Peak Volcano in the North Cascade Range of Washington deposited volcanic tephra (layers B, G, and M) over a widespread area east of the vent (Porter 1978). One of these geochemically distinguishable eruptive events resulted in the deposition of Layer G about 11,200 B.P. (Foit et al. 1993; Mehringer et al. 1984). Minor deposition of tephra during the last 6,000 years (layers A, D, and X), confined to local areas surrounding the eruptive vent, are reported by Beget (1981).

**Mount St. Helens, Washington.** During the last 40,000 years, Mount St. Helens in the southern Washington Cascades has been a prolific source of ash fall. More than 100 explosive eruptive events have been identified, based on various ash beds, layers, and sets found in environments downwind from the volcano. The tephra sets consist of individual beds and layers that are stratigraphically, temporally, mineralogically, or chemically distinguished from adjacent sets. Mount St. Helens tephra sets B, D, J, P, S, T, W, X, and Y have been correlated with Holocene or very late Pleistocene volcanic activity (Mullineaux 1986).

**Mount Hood, Oregon.** Pumice and ash deposits resulting from late Holocene eruptions at Mount Hood in the Oregon Cascades have been reported by Crandell (1980). However, the geographic distribution of the tephra deposits is not well known and appears to be confined to the vicinity of the volcano.

**South Sister, Oregon.** Eruptive activity about 2,000 $^{14}C$ years ago on the southern and southeastern flanks of South Sister Volcano spread volcanic ash and lapilli several tens of kilometers to the east and southeast of the vents (Scott 1987; Skinner and Radosevich 1991). Although the thickness of the deposits diminishes rapidly to the east of the vents, tephra may be present in favorable environments along segments of the Pipeline transect immediately east of the vents; however, none were observed during the Project.

**Newberry Volcano, Oregon.** The collapsed caldera of Newberry Volcano is located 18 km (11 mi) east of the pipeline corridor near Lapine, Oregon. Explosive eruptions of ash and lapilli preceded extrusion of the Big Obsidian Flow, which has been dated at approximately 1,350 $^{14}C$ years (Jensen 1988). Deposits of ash and lapilli from the eruption spread to the east of the vent as a narrow lobe and to the west as a thin veneer. Other Pleistocene and early Holocene deposits of tephra at Newberry Volcano are largely associated with sources within the caldera and have been poorly mapped and dated (Jensen 1988).

**Mount Mazama, Oregon.** The thickest and most widespread tephra deposits encountered in the Project area originated from the pre-climactic and climactic explosive eruptions of Mount Mazama that formed Crater Lake in the southern Oregon Cascades. All but the southernmost portion of the PEP corridor falls within the known boundaries of ash resulting

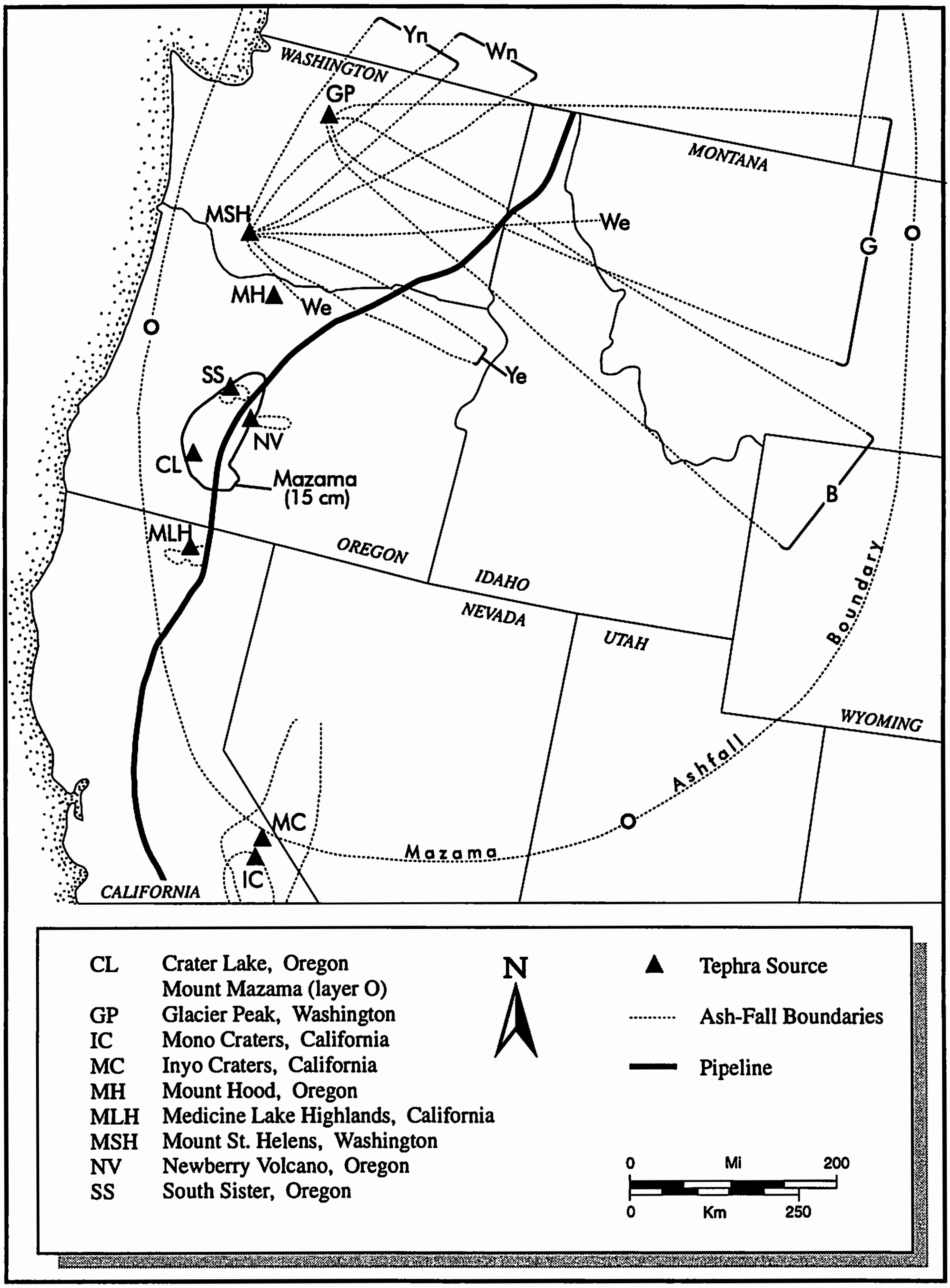


Figure 7-2 Major Holocene sources of volcanic tephra in the far western United States (adapted from Sarna-Wojcicki et al. 1983:56).

from these massive eruptions. Deposits of Mazama tephra, sometimes designated in the literature as the "O layer," have been found as a discrete bed as far away as Lec la Biche, Alberta, over 1,550 km northeast of Crater Lake (Westgate and Briggs 1980). The age of the Mazama ash-fall is well documented (Bacon 1983). The weighted mean average of four carbon samples associated with the climactic eruptions are reported as 6,845 $\pm$ 50 $^{14}C$ years, which is the date most commonly cited in the literature for the climactic eruptions of Mount Mazama (Bacon 1983; Skinner and Radosevich 1991). The eruptive history of Mount Mazama and its possible effects on prehistoric populations is described by Bacon (1983), Matz (1991), and Skinner and Radosevich (1991).

**Medicine Lake Highlands, California.** Late Holocene eruptive activity in the Medicine Lake Highlands of northern California resulted in the extrusion of several obsidian flows and the deposition of associated volcanic tephra deposits. Two of the most widespread and best documented tephra deposits originated almost contemporaneously from vents that are capped by the Little Glass Mountain and nearby Glass Mountain obsidian flows. Paleomagnetic measurements and radiocarbon dates from charred wood place the time of the Glass Mountain eruption at about 850-900 B.P. (Heiken 1978). Tephra from these eruptions was deposited downwind to the east and is found in surficial deposits in the pipeline corridor. The Little Glass Mountain eruptions preceded those at Glass Mountain by only a short period and are estimated to have occurred between 900 and 1,050 years ago (Donnelly-Nolan et al. 1990; Heiken 1978). Airfall ash deposits from Little Glass Mountain are confined to the local Medicine Lake Highlands region and probably do not extend into the Project corridor.

**Pleistocene Tephra Deposits.** In addition to the Holocene tephra sources that are well documented and used by archaeologists, many Pleistocene sources and tephra deposits have been documented in the Project area from core samples collected from numerous lakes, bogs, and lacustrine sediments. These data are summarized by Davis (1985) and Sarna-Wojcicki et al (1987, 1991).

## 7.3 METHODS

Selected volcanic tephra samples were submitted to Dr. Franklin F. Foit, Department of Geology, Washington State University, for analysis using electron microprobe characterization and for comparison with known data bases containing geologic source information. The results of the 1992-1993 analyses are presented in the letter reports at the end of this section and are summarized in Tables 7-2 and 7-3. Letter reports by Dr. Foit describing earlier PEP tephra analyses are presented in Lebow et al. (1991) and Speulda et al. (1992).

### 7.3.1 Sample Collection and Preparation

Tephra samples collected in the field typically were bagged separately and labeled as volcanic ash samples. No special sample collection methods were required. Whenever possible, the samples were identified as primary or redeposited. In preparation for electron microprobe analysis, a small subset of the collected volcanic tephra was dispersed in epoxy on a glass slide, polished, and carbon coated. Sample preparation and other analytical details are described by Foit et al. (1993).

Table 7-2 Summary of Volcanic Tephra Characterization Studies.

| Site | Lot-Spec | Ash[a] | Unit | | | Depth (cm) | | Tephra Source | Comments |
|---|---|---|---|---|---|---|---|---|---|
| CA-MOD-2561 | 24 - 149 | A | T-2561-1 | 2.00 S | 13.00 E | -35.00 | -35.00 | Medicine Lake Highlands | Probable Glass Mountain tephra |
| CA-MOD-2573 | 204 - 1 | A | TEU 1 | 0.00 S | 0.00 E | -100.00 | -110.00 | Mazama? | Probable Mazama |
| CA-MOD-2573 | 204 - 1 | B | TEU 1 | 0.00 S | 0.00 E | -110.00 | -100.00 | Unknown | Similar to Olema Bed |
| 10-BY-309 | 74 - 2 | A | SON 12 | 0.00 S | 0.00 E | -40.00 | -50.00 | Mazama | - |
| 10-BY-309 | 115 - 1 | A | TEU 2 | 0.00 S | 0.00 E | -52.00 | -52.00 | Mazama | - |
| 35-DS-263 | 958 - 1 | A | TEU 2 | 0.00 S | 0.00 E | -190.00 | -200.00 | Unknown | Pre-Mazama |
| 35-DS-557 | 2276 - 1 | A | BHT 8 | 0.00 S | 0.00 E | -133.00 | -143.00 | Unknown | Similar to Clear Lake/Summer Lake |
| 35-DS-557 | 2276 - 1 | B | BHT 8 | 0.00 S | 0.00 E | -133.00 | -143.00 | Unknown | Similar to Summer Lake |
| 35-GM-25 | 286 - 1 | A | TEU 2 | 0.00 S | 0.00 E | -103.00 | -103.00 | Mazama | - |
| 35-GM-25 | 1424 - 1 | A | EXU | 107.00 S | 125.00 E | -138.00 | -142.00 | Mazama | - |
| 35-GM-103 | 50 - 1 | A | SON 6 | 0.00 S | 0.00 E | -60.00 | -60.00 | Mazama | - |
| 35-JE-49 | 271 - 1 | A | TEU 3 | 0.00 S | 0.00 E | -130.00 | -130.00 | Mazama | - |
| 35-JE-49 | 276 - 1 | A | PIT 1 | 0.00 S | 0.00 E | -102.00 | -102.00 | Mazama | - |
| 35-JE-49 | 276 - 1 | B | PIT 1 | 0.00 S | 0.00 E | -102.00 | -102.00 | High-Potassium Unknown | Potassium-rich glass |
| 35-JE-49 | 276 - 1 | C | PIT 1 | 0.00 S | 0.00 E | -102.00 | -102.00 | Unknown | - |
| 35-JE-49 | 280 - 1 | A | TEU 1 | 0.00 S | 0.00 E | -126.00 | -130.00 | Mazama | - |
| 35-JE-49 | 1462 - 1 | A | EXU | 18.00 S | 13.00 E | -248.00 | -262.00 | Mazama | - |
| 35-JE-49 | 1464 - 2 | A | EXU | 18.00 S | 13.00 E | -244.00 | -248.00 | Mazama | - |
| 35-JE-49 | 1467 - 2 | A | EXU | 18.00 S | 13.00 E | -233.00 | -235.00 | Mazama | - |
| 35-JE-49 | 1469 - 2 | A | EXU | 18.00 S | 13.00 E | -228.00 | -231.00 | Mazama | - |
| 35-JE-49 | 1592 - 1 | A | MEC 1 | 0.00 S | 0.00 E | -150.00 | -150.00 | Unknown | - |
| 35-JE-49 | 1592 - 1 | B | MEC 1 | 0.00 S | 0.00 E | -150.00 | -150.00 | Unknown | - |
| 35-JE-49 | 1592 - 1 | C | MEC 1 | 0.00 S | 0.00 E | -150.00 | -150.00 | Unknown | - |
| 35-JE-49 | 1592 - 1 | D | MEC 1 | 0.00 S | 0.00 E | -150.00 | -150.00 | Unknown | - |
| 35-JE-49 | 1592 - 1 | E | MEC 1 | 0.00 S | 0.00 E | -150.00 | -150.00 | Unknown | - |
| 35-JE-49 | 1592 - 1 | F | MEC 1 | 0.00 S | 0.00 E | -150.00 | -150.00 | John Day Formation | Potassium-rich glass |
| 35-JE-50 | 85 - 1 | A | AUG 43 | 0.00 S | 0.00 E | -120.00 | -140.00 | Mazama | - |
| 35-JE-50 | 85 - 1 | B | AUG 43 | 0.00 S | 0.00 E | -120.00 | -140.00 | John Day Formation | Potassium-rich glass |
| 35-JE-50 | 85 - 2 | A | AUG 43 | 0.00 S | 0.00 E | -120.00 | -140.00 | Mazama | - |

[a] Geochemically distinguishable group(s) identified in an individual sample, e.g., A = geochemical group 1; B = geochemical group 2.

Table 7-2 (continued)

| Site | Lot-Spec | Ash[a] | Unit | | | | Depth (cm) | | Tephra Source | Comments |
|---|---|---|---|---|---|---|---|---|---|---|
| 35-JE-51B | 84 - 1 | A | SOX | 2 | 0.00 S | 0.00 E | -230.00 | -230.00 | Mazama | - |
| 35-JE-51B | 84 - 1 | B | SOX | 2 | 0.00 S | 0.00 E | -230.00 | -230.00 | John Day Formation | Potassium-rich glass |
| 35-JE-51B | 130 - 1 | A | SOX | 6 | 0.00 S | 0.00 E | -220.00 | -225.00 | Mazama | - |
| 35-JE-51B | 130 - 1 | B | SOX | 6 | 0.00 S | 0.00 E | -220.00 | -225.00 | John Day Formation | Potassium-rich glass |
| 35-JE-51B | 245 - 1 | A | TEU | 4 | 0.00 S | 0.00 E | -137.00 | -137.00 | Mazama | - |
| 35-JE-51B | 245 - 1 | B | TEU | 4 | 0.00 S | 0.00 E | -137.00 | -137.00 | John Day Formation | Potassium-rich glass |
| 35-JE-51B | 259 - 1 | A | TEX | 4 | 0.00 S | 0.00 E | -300.00 | -305.00 | Mazama | - |
| 35-JE-51B | 259 - 1 | B | TEX | 4 | 0.00 S | 0.00 E | -300.00 | -305.00 | John Day Formation | Potassium-rich glass |
| 35-JE-51B | 1014 - 1 | A | MEC | 1 | 88.00 S | 70.00 E | 0.00 | 0.00 | John Day Formation | Potassium-rich glass |
| 35-JE-51B | 1014 - 1 | B | MEC | 1 | 88.00 S | 70.00 E | 0.00 | 0.00 | High-Potassium Unknown | Potassium-rich glass |
| 35-JE-51B | 1014 - 1 | C | MEC | 1 | 88.00 S | 70.00 E | 0.00 | 0.00 | Mazama | - |
| 35-JE-51B | 1015 - 1 | A | MEC | 2 | 107.00 S | 75.00 E | -156.00 | -156.00 | John Day Formation | Potassium-rich glass |
| 35-JE-51B | 1015 - 1 | B | MEC | 2 | 107.00 S | 75.00 E | -156.00 | -156.00 | High-Potassium Unknown | Potassium-rich glass |
| 35-JE-51B | 1015 - 1 | C | MEC | 2 | 107.00 S | 75.00 E | -156.00 | -156.00 | Mazama | - |
| 35-JE-51B | 1016 - 1 | A | EXU | | 125.50 S | 100.50 E | -190.00 | -196.00 | Mazama | - |
| 35-JE-51B | 1017 - 1 | A | EXU | | 102.00 S | 83.00 E | -116.00 | -116.00 | John Day Formation | Potassium-rich glass |
| 35-JE-51B | 1017 - 1 | B | EXU | | 102.00 S | 83.00 E | -116.00 | -116.00 | High-Potassium Unknown | Potassium-rich glass |
| 35-JE-51B | 2350 - 2 | A | EXU | | 112.00 S | 90.00 E | -152.00 | -154.00 | John Day Formation | Potassium-rich glass |
| 35-JE-51B | 2350 - 2 | B | EXU | | 112.00 S | 90.00 E | -152.00 | -154.00 | High-Potassium Unknown | Potassium-rich glass |
| 35-JE-51B | 2350 - 2 | C | EXU | | 112.00 S | 90.00 E | -152.00 | -154.00 | High-Potassium Unknown | Potassium-rich glass |
| 35-JE-51B | 2763 - 2 | A | EXU | | 123.00 S | 84.00 E | -223.00 | -226.00 | Mazama | Potassium-rich glass |
| 35-JE-51B | 2763 - 2 | B | EXU | | 123.00 S | 84.00 E | -223.00 | -226.00 | John Day Formation | Potassium-rich glass |
| 35-JE-51B | 3932 - 1 | A | SCN | 1 | 0.00 S | 0.00 E | 0.00 | 0.00 | John Day Formation | John Day Formation geologic sample |
| 35-JE-51B | 3932 - 1 | B | SCN | 1 | 0.00 S | 0.00 E | 0.00 | 0.00 | John Day Formation | John Day Formation geologic sample |
| 35-JE-51B | 3932 - 1 | C | SCN | 1 | 0.00 S | 0.00 E | 0.00 | 0.00 | John Day Formation | John Day Formation geologic sample |
| 35-JE-51B | 3932 - 1 | D | SCN | 1 | 0.00 S | 0.00 E | 0.00 | 0.00 | John Day Formation | John Day Formation geologic sample |
| 35-JE-51B | 3932 - 1 | E | SCN | 1 | 0.00 S | 0.00 E | 0.00 | 0.00 | John Day Formation | John Day Formation geologic sample |
| 35-JE-283 | 187 - 1 | A | TEU | 3 | 0.00 S | 0.00 E | -100.00 | -110.00 | Mazama | - |
| 35-JE-283 | 187 - 1 | B | TEU | 3 | 0.00 S | 0.00 E | -100.00 | -110.00 | John Day Formation | Potassium-rich glass |

[a] Geochemically distinguishable group(s) identified in an individual sample, e.g., A = geochemical group 1; B = geochemical group 2.

Table 7-2 (continued)

| Site | Lot-Spec | Ash[a] | Unit | | | | Depth (cm) | | Tephra Source | Comments |
|---|---|---|---|---|---|---|---|---|---|---|
| 35-JE-283 | 398 - 2 | A | EXU | | 86.00 S | 103.00 E | -108.00 | -110.00 | Mazama | - |
| 35-JE-283 | 398 - 2 | B | EXU | | 86.00 S | 103.00 E | -108.00 | -110.00 | John Day Formation | Potassium-rich glass |
| 35-JE-283 | 439 - 2 | A | EXU | | 87.00 S | 93.00 E | -90.00 | -95.00 | Mazama | - |
| 35-JE-283 | 439 - 2 | B | EXU | | 87.00 S | 93.00 E | -90.00 | -95.00 | John Day Formation | Potassium-rich glass |
| 35-JE-283 | 916 - 1 | A | MEC | 4 | 150.00 S | 71.50 E | -110.00 | -110.00 | Unknown | - |
| 35-JE-283 | 916 - 1 | B | MEC | 4 | 150.00 S | 71.50 E | -110.00 | -110.00 | John Day Formation | Potassium-rich glass |
| 35-JE-283 | 916 - 1 | C | MEC | 4 | 150.00 S | 71.50 E | -110.00 | -110.00 | Unknown | - |
| 35-JE-288 | 277 - 1 | A | TEX | 1 | 0.00 S | 0.00 E | -210.10 | -228.00 | Mazama | - |
| 35-JE-288 | 277 - 1 | B | TEX | 1 | 0.00 S | 0.00 E | -210.10 | -228.00 | John Day Formation | Potassium-rich glass |
| 35-JE-289 | 46 - 1 | A | SHX | 10 | 0.00 S | 0.00 E | -100.00 | -120.00 | Mazama | - |
| 35-JE-296 | 411 - 1 | A | TEU | 2 | 0.00 S | 0.00 E | -30.00 | -40.00 | Mazama | - |
| 35-JE-298 | 301 - 3 | A | TEU | 3 | 0.00 S | 0.00 E | -180.00 | -190.00 | Mazama | - |
| 35-SH-134 | 15 - 1 | A | SHP | 2 | 0.00 S | 0.00 E | -60.00 | -80.00 | Mazama | - |
| 35-SH-134 | 20 - 1 | A | SHP | 3 | 0.00 S | 0.00 E | 0.00 | -20.00 | Mazama | - |
| 35-SH-134 | 22 - 2 | A | SHP | 3 | 0.00 S | 0.00 E | -40.00 | -60.00 | Mazama | - |
| 35-UM-154 | 323 - 1 | A | TRENCH | | 83.00 S | 100.00 E | -92.00 | -98.00 | Mazama | - |
| 35-UM-154 | 323 - 1 | B | TRENCH | | 83.00 S | 100.00 E | -92.00 | -98.00 | Glacier Peak | 11,200 B.P. eruption |
| 35-UM-154 | 324 - 1 | A | TRENCH | | 83.00 S | 100.00 E | -107.50 | -112.50 | Mazama | - |
| 35-UM-154 | 324 - 1 | B | TRENCH | | 83.00 S | 100.00 E | -107.50 | -112.50 | Glacier Peak | 11,200 B.P. eruption |
| 35-UM-154 | 326 - 1 | A | TRENCH | | 83.00 S | 100.00 E | -93.00 | -97.00 | Mazama | - |
| 35-UM-154 | 326 - 1 | B | TRENCH | | 83.00 S | 100.00 E | -93.00 | -97.00 | Unknown | Similar to Trego Hot Springs tephra |
| 35-WS-120 | 395 - 1 | C | TEU | 1 | 0.00 S | 0.00 E | -38.00 | -40.00 | Mazama | - |
| 35-WS-120 | 412 - 1 | A | TEU | 1 | 0.00 S | 0.00 E | -30.00 | -40.00 | Mazama | - |
| 35-WS-120 | 444 - 1 | A | TEU | 2 | 0.00 S | 0.00 E | -133.00 | -133.00 | Unknown | May be same group as 444-C |
| 35-WS-120 | 444 - 1 | B | TEU | 2 | 0.00 S | 0.00 E | -133.00 | -133.00 | Mount St. Helens | Similar to sets Ye, We, Jy, S |
| 35-WS-120 | 444 - 1 | C | TEU | 2 | 0.00 S | 0.00 E | -133.00 | -133.00 | Unknown | May be same group as 444-1A |
| 35-WS-120 | 444 - 1 | D | TEU | 2 | 0.00 S | 0.00 E | -133.00 | -133.00 | Unknown | - |
| 35-WS-120 | 444 - 1 | E | TEU | 2 | 0.00 S | 0.00 E | -133.00 | -133.00 | Unknown | - |
| 35-WS-223 | 26 - 1 | A | STU | 2 | 0.00 S | 0.00 E | -12.00 | -12.00 | Mazama | - |

[a] Geochemically distinguishable group(s) identified in an individual sample, e.g., A = geochemical group 1; B = geochemical group 2.

Table 7-2 (continued)

| Site | Lot-Spec | Ash[a] | Unit | | | | Depth (cm) | | Tephra Source | Comments |
|---|---|---|---|---|---|---|---|---|---|---|
| 35-WS-223 | 26 - 1 | B | STU | 2 | 0.00 S | 0.00 E | -12.00 | -12.00 | John Day Formation | Potassium-rich glass |
| 35-WS-225 | 134 - 1 | A | TEU | 3 | 0.00 S | 0.00 E | -45.00 | -60.00 | Mazama | - |
| 35-WS-225 | 187 - 1 | A | TEX | 7 | 0.00 S | 0.00 E | -200.00 | -220.00 | Mazama | - |
| 35-WS-225 | 217 - 1 | A | TEU | 9 | 0.00 S | 0.00 E | -50.00 | -54.00 | Mazama | - |
| 35-WS-225 | 258 - 1 | A | EXU | | 100.00 S | 158.00 E | -129.00 | -129.00 | Mazama | - |
| 35-WS-226 | 100 - 1 | A | STU | 4 | 0.00 S | 0.00 E | -10.00 | -20.00 | Mazama | - |
| 35-WS-230 | 218 - 1 | A | TEU | 2 | 0.00 S | 0.00 E | -70.00 | -85.00 | Mazama | - |
| 35-WS-231 | 421 - 1 | A | TEU | 2 | 0.00 S | 0.00 E | -140.00 | -140.00 | Mazama | - |
| 35-WS-231 | 424 - 1 | A | TEU | 2 | 0.00 S | 0.00 E | -150.00 | -150.00 | Mazama | - |
| 35-WS-231 | 427 - 1 | A | TEU | 2 | 0.00 S | 0.00 E | -150.00 | -160.00 | Mazama | - |
| 35-WS-232 | 46 - 1 | A | STU | 4 | 0.00 S | 0.00 E | 0.00 | -10.00 | Mazama | - |
| 45-WW-100 | 207 - 1 | A | BHT | 1 | 0.00 S | 0.00 E | -104.00 | -104.00 | Glacier Peak | - |
| 45-WW-100 | 213 - 1 | A | E.BLWT | 1 | 0.00 S | 0.00 E | -20.00 | -36.00 | Mazama | - |
| 45-WW-101 | 2 - 1 | A | GEO | 1 | 0.00 S | 0.00 E | 0.00 | 0.00 | Mazama | - |

[a] Geochemically distinguishable group(s) identified in an individual sample, e.g., A = geochemical group 1; B = geochemical group 2.

## Table 7-3 Results of Electron Microprobe Analyses of Volcanic Tephra Samples.

| Site | Specimen | Ash [a] | Chemical Composition | | | | | | | | | | | Tephra Source |
|---|---|---|---|---|---|---|---|---|---|---|---|---|---|---|
| | | | $SiO_2$ | $Al_2O_3$ | $Fe_2O_3$ | $TiO_2$ | $Na_2O$ | $K_2O$ | MgO | CaO | Cl | Total | N= | |
| CA-MOD-2561 | 24 - 149 | A | 73.62 | 13.98 | 2.15 | 0.31 | 3.96 | 4.23 | 0.30 | 1.38 | 0.07 | 100 | 21 | Medicine Lake Highlands |
| CA-MOD-2573 | 204 - 1 | A | 73.77 | 14.01 | 2.33 | 0.30 | 4.52 | 2.98 | 0.38 | 1.56 | 0.15 | 100 | 4 | Mazama? |
| CA-MOD-2573 | 204 - 1 | B | 75.37 | 13.27 | 1.97 | 0.22 | 4.44 | 3.96 | 0.10 | 0.51 | 0.16 | 100 | 6 | Unknown |
| 10-BY-309 | 74 - 2 | A | 73.07 | 14.44 | 2.21 | 0.41 | 4.92 | 2.69 | 0.44 | 1.64 | 0.18 | 100 | 23 | Mazama |
| 10-BY-309 | 115 - 1 | A | 72.79 | 14.47 | 2.35 | 0.45 | 5.00 | 2.69 | 0.48 | 1.59 | 0.18 | 100 | 6 | Mazama |
| 35-DS-263 | 958 - 1 | A | 75.05 | 13.11 | 1.98 | 0.15 | 4.80 | 4.17 | 0.10 | 0.49 | 0.15 | 100 | 21 | Unknown |
| 35-DS-557 | 2276 - 1 | A | 75.25 | 13.24 | 1.73 | 0.17 | 4.63 | 4.19 | 0.10 | 0.54 | 0.15 | 100 | 20 | Unknown |
| 35-DS-557 | 2276 - 1 | B | 69.99 | 14.83 | 3.88 | 0.53 | 5.63 | 2.85 | 0.53 | 1.64 | 0.10 | 100 | 2 | Unknown |
| 35-GM-25 | 286 - 1 | A | 72.87 | 14.40 | 2.43 | 0.40 | 5.00 | 2.69 | 0.45 | 1.60 | 0.17 | 100 | 15 | Mazama |
| 35-GM-25 | 1424 - 1 | A | 73.18 | 14.38 | 2.27 | 0.42 | 4.74 | 2.71 | 0.46 | 1.65 | 0.19 | 100 | 17 | Mazama |
| 35-GM-103 | 50 - 1 | A | 73.14 | 14.23 | 2.48 | 0.41 | 4.91 | 2.64 | 0.47 | 1.56 | 0.17 | 100 | 17 | Mazama |
| 35-JE-49 | 271 - 1 | A | 72.81 | 14.36 | 2.43 | 0.43 | 5.03 | 2.68 | 0.46 | 1.61 | 0.19 | 100 | 17 | Mazama |
| 35-JE-49 | 276 - 1 | A | 72.93 | 14.29 | 2.31 | 0.40 | 4.85 | 2.98 | 0.45 | 1.63 | 0.16 | 100 | 26 | Mazama |
| 35-JE-49 | 276 - 1 | B | 70.64 | 14.03 | 2.27 | 0.40 | 1.04 | 9.48 | 0.42 | 1.57 | 0.15 | 100 | 8 | High-Potassium Unknown |
| 35-JE-49 | 276 - 1 | C | 75.98 | 12.91 | 1.68 | 0.11 | 4.12 | 4.14 | 0.14 | 0.80 | 0.12 | 100 | 2 | Unknown |
| 35-JE-49 | 280 - 1 | A | 72.69 | 14.35 | 2.50 | 0.43 | 5.10 | 2.67 | 0.45 | 1.63 | 0.18 | 100 | 16 | Mazama |
| 35-JE-49 | 1462 - 1 | A | 73.12 | 14.47 | 2.00 | 0.47 | 5.05 | 2.66 | 0.46 | 1.60 | 0.17 | 100 | 16 | Mazama |
| 35-JE-49 | 1464 - 2 | A | 73.20 | 14.52 | 2.02 | 0.41 | 4.96 | 2.66 | 0.46 | 1.60 | 0.17 | 100 | 15 | Mazama |
| 35-JE-49 | 1467 - 2 | A | 73.28 | 14.46 | 1.98 | 0.41 | 4.94 | 2.67 | 0.45 | 1.59 | 0.21 | 100 | 13 | Mazama |
| 35-JE-49 | 1469 - 2 | A | 73.34 | 14.48 | 1.99 | 0.43 | 4.81 | 2.69 | 0.46 | 1.61 | 0.19 | 100 | 17 | Mazama |
| 35-JE-49 | 1592 - 1 | A | 75.31 | 13.28 | 1.91 | 0.18 | 4.38 | 4.11 | 0.11 | 0.57 | 0.15 | 100 | 12 | Unknown |
| 35-JE-49 | 1592 - 1 | B | 76.63 | 13.68 | 1.19 | 0.12 | 3.86 | 2.44 | 0.27 | 1.72 | 0.09 | 100 | 9 | Unknown |
| 35-JE-49 | 1592 - 1 | C | 76.37 | 13.41 | 1.38 | 0.17 | 3.88 | 3.20 | 0.23 | 1.22 | 0.14 | 100 | 5 | Unknown |
| 35-JE-49 | 1592 - 1 | D | 74.84 | 13.82 | 2.20 | 0.26 | 4.33 | 2.40 | 0.34 | 1.62 | 0.19 | 100 | 5 | Unknown |
| 35-JE-49 | 1592 - 1 | E | 72.83 | 14.09 | 2.99 | 0.45 | 4.52 | 3.64 | 0.27 | 1.11 | 0.10 | 100 | 3 | Unknown |
| 35-JE-49 | 1592 - 1 | F | 76.28 | 12.14 | 2.74 | 0.17 | 2.84 | 5.15 | 0.03 | 0.50 | 0.15 | 100 | 2 | John Day Formation |
| 35-JE-50 | 85 - 1 | A | 72.69 | 14.40 | 2.43 | 0.42 | 5.14 | 2.69 | 0.46 | 1.60 | 0.17 | 100 | 20 | Mazama |
| 35-JE-50 | 85 - 1 | B | 76.01 | 12.19 | 2.63 | 0.15 | 2.42 | 5.71 | 0.02 | 0.78 | 0.09 | 100 | 10 | John Day Formation |

Major element results are reported in weight percent oxide; results are an average value of multiple analyses (see N= for the number of tephra shards analyzed).

[a] Geochemically distinguishable group(s) identified in an individual sample, e.g., A = geochemical group 1; B = geochemical group 2.

Table 7-3 (continued)

| Site | Specimen | Ash[a] | Chemical Composition | | | | | | | | | | | Tephra Source |
|---|---|---|---|---|---|---|---|---|---|---|---|---|---|---|
| | | | $SiO_2$ | $Al_2O_3$ | $Fe_2O_3$ | $TiO_2$ | $Na_2O$ | $K_2O$ | MgO | CaO | Cl | Total | N= | |
| 35-JE-50 | 85-2 | A | 72.68 | 14.41 | 2.34 | 0.40 | 5.17 | 2.68 | 0.46 | 1.66 | 0.18 | 100 | 17 | Mazama |
| 35-JE-51B | 84-1 | A | 72.58 | 14.42 | 2.42 | 0.41 | 5.22 | 2.68 | 0.46 | 1.63 | 0.18 | 100 | 15 | Mazama |
| 35-JE-51B | 84-1 | B | 76.12 | 12.21 | 2.59 | 0.20 | 2.14 | 5.89 | 0.03 | 0.75 | 0.07 | 100 | 14 | John Day Formation |
| 35-JE-51B | 130-1 | A | 73.00 | 14.46 | 2.21 | 0.43 | 4.96 | 2.70 | 0.46 | 1.61 | 0.17 | 100 | 16 | Mazama |
| 35-JE-51B | 130-1 | B | 75.96 | 12.20 | 2.62 | 0.17 | 2.53 | 5.57 | 0.03 | 0.79 | 0.13 | 100 | 13 | John Day Formation |
| 35-JE-51B | 245-1 | A | 73.08 | 14.33 | 2.29 | 0.42 | 4.96 | 2.69 | 0.45 | 1.60 | 0.18 | 100 | 12 | Mazama |
| 35-JE-51B | 245-1 | B | 76.18 | 12.15 | 2.56 | 0.19 | 2.23 | 5.87 | 0.02 | 0.74 | 0.06 | 100 | 12 | John Day Formation |
| 35-JE-51B | 259-1 | A | 72.83 | 14.39 | 2.40 | 0.41 | 5.07 | 2.70 | 0.45 | 1.59 | 0.16 | 100 | 17 | Mazama |
| 35-JE-51B | 259-1 | B | 76.28 | 12.15 | 2.63 | 0.19 | 2.11 | 5.81 | 0.03 | 0.74 | 0.06 | 100 | 11 | John Day Formation |
| 35-JE-51B | 1014-1 | A | 76.27 | 12.07 | 2.53 | 0.21 | 2.07 | 5.94 | 0.02 | 0.81 | 0.08 | 100 | 18 | John Day Formation |
| 35-JE-51B | 1014-1 | B | 75.58 | 11.99 | 2.47 | 0.16 | 0.66 | 8.32 | 0.02 | 0.76 | 0.04 | 100 | 7 | High-Potassium Unknown |
| 35-JE-51B | 1014-1 | C | 72.84 | 14.43 | 2.14 | 0.42 | 4.81 | 2.67 | 0.49 | 1.72 | 0.48 | 100 | 1 | Mazama |
| 35-JE-51B | 1015-1 | A | 76.22 | 12.12 | 2.42 | 0.20 | 2.25 | 5.90 | 0.02 | 0.80 | 0.07 | 100 | 12 | John Day Formation |
| 35-JE-51B | 1015-1 | B | 75.24 | 12.03 | 2.42 | 0.17 | 0.44 | 8.88 | 0.03 | 0.71 | 0.08 | 100 | 7 | High-Potassium Unknown |
| 35-JE-51B | 1015-1 | C | 73.17 | 14.31 | 2.22 | 0.39 | 4.80 | 2.69 | 0.49 | 1.73 | 0.20 | 100 | 7 | Mazama |
| 35-JE-51B | 1016-1 | A | 72.76 | 14.25 | 2.47 | 0.46 | 5.17 | 2.70 | 0.45 | 1.58 | 0.16 | 100 | 16 | Mazama |
| 35-JE-51B | 1017-1 | A | 76.12 | 12.15 | 2.58 | 0.21 | 2.09 | 5.99 | 0.05 | 0.75 | 0.06 | 100 | 16 | John Day Formation |
| 35-JE-51B | 1017-1 | B | 74.02 | 12.63 | 2.44 | 0.27 | 0.41 | 9.00 | 0.16 | 0.99 | 0.08 | 100 | 8 | High-Potassium Unknown |
| 35-JE-51B | 2350-2 | A | 76.29 | 12.28 | 2.25 | 0.21 | 2.22 | 5.85 | 0.04 | 0.80 | 0.08 | 100 | 10 | John Day Formation |
| 35-JE-51B | 2350-2 | B | 75.31 | 12.15 | 2.20 | 0.17 | 0.10 | 9.20 | 0.03 | 0.79 | 0.05 | 100 | 9 | High-Potassium Unknown |
| 35-JE-51B | 2350-2 | C | 77.10 | 12.53 | 1.50 | 0.19 | 1.43 | 4.66 | 0.26 | 2.31 | 0.02 | 100 | 3 | High-Potassium Unknown |
| 35-JE-51B | 2763-2 | A | 73.05 | 14.47 | 2.10 | 0.44 | 5.05 | 2.66 | 0.44 | 1.60 | 0.19 | 100 | 9 | Mazama |
| 35-JE-51B | 2763-2 | B | 76.39 | 12.30 | 2.20 | 0.17 | 2.27 | 5.86 | 0.26 | 2.31 | 0.02 | 100 | 14 | John Day Formation |
| 35-JE-51B | 3932-1 | A | 76.40 | 12.20 | 2.16 | 0.19 | 2.45 | 5.80 | 0.02 | 0.76 | 0.08 | 100 | 39 | John Day Formation |
| 35-JE-51B | 3932-1 | B | 76.08 | 12.14 | 2.48 | 0.19 | 2.60 | 5.68 | 0.03 | 0.71 | 0.07 | 100 | 28 | John Day Formation |
| 35-JE-51B | 3932-1 | C | 77.41 | 12.40 | 1.10 | 0.17 | 1.94 | 6.19 | 0.07 | 0.68 | 0.04 | 100 | 9 | John Day Formation |
| 35-JE-51B | 3932-1 | D | 76.38 | 12.13 | 2.38 | 0.19 | 2.28 | 5.87 | 0.03 | 0.69 | 0.05 | 100 | 20 | John Day Formation |
| 35-JE-51B | 3932-1 | E | 75.78 | 11.98 | 2.61 | 0.19 | 3.36 | 5.21 | 0.02 | 0.72 | 0.13 | 100 | 8 | John Day Formation |

Major element results are reported in weight percent oxide; results are an average value of multiple analyses (see N= for the number of tephra shards analyzed).

[a] Geochemically distinguishable group(s) identified in an individual sample, e.g., A = geochemical group 1; B = geochemical group 2.

Table 7-3 (continued)

| Site | Specimen | Ash[a] | Chemical Composition | | | | | | | | | | | Tephra Source |
|---|---|---|---|---|---|---|---|---|---|---|---|---|---|---|
| | | | $SiO_2$ | $Al_2O_3$ | $Fe_2O_3$ | $TiO_2$ | $Na_2O$ | $K_2O$ | MgO | CaO | Cl | Total | N= | |
| 35-JE-283 | 187 - 1 | A | 72.87 | 14.39 | 2.39 | 0.44 | 5.08 | 2.62 | 0.45 | 1.58 | 0.19 | 100 | 16 | Mazama |
| 35-JE-283 | 187 - 1 | B | 76.24 | 12.08 | 2.55 | 0.20 | 2.02 | 6.09 | 0.44 | 0.68 | 0.13 | 100 | 11 | John Day Formation |
| 35-JE-283 | 398 - 2 | A | 73.14 | 14.48 | 2.21 | 0.45 | 4.94 | 2.61 | 0.45 | 1.59 | 0.16 | 100 | 17 | Mazama |
| 35-JE-283 | 398 - 2 | B | 76.31 | 12.25 | 2.29 | 0.18 | 2.16 | 6.00 | 0.02 | 0.66 | 0.13 | 100 | 12 | John Day Formation |
| 35-JE-283 | 439 - 2 | A | 73.09 | 14.48 | 2.17 | 0.41 | 4.94 | 2.69 | 0.45 | 1.61 | 0.16 | 100 | 16 | Mazama |
| 35-JE-283 | 439 - 2 | B | 76.25 | 12.23 | 2.44 | 0.21 | 2.12 | 5.95 | 0.02 | 0.66 | 0.12 | 100 | 12 | John Day Formation |
| 35-JE-283 | 916 - 1 | A | 72.37 | 14.54 | 2.86 | 0.30 | 4.85 | 3.35 | 0.32 | 1.29 | 0.12 | 100 | 2 | Unknown |
| 35-JE-283 | 916 - 1 | B | 76.24 | 12.20 | 2.35 | 0.18 | 2.45 | 5.77 | 0.02 | 0.64 | 0.15 | 100 | 13 | John Day Formation |
| 35-JE-283 | 916 - 1 | C | 73.84 | 14.06 | 2.21 | 0.20 | 4.83 | 3.76 | 0.14 | 0.87 | 0.09 | 100 | 10 | Unknown |
| 35-JE-288 | 277 - 1 | A | 72.79 | 14.43 | 2.41 | 0.42 | 5.12 | 2.62 | 0.45 | 1.59 | 0.17 | 100 | 18 | Mazama |
| 35-JE-288 | 277 - 1 | B | 76.16 | 12.08 | 2.60 | 0.17 | 2.42 | 5.75 | 0.45 | 0.67 | 0.12 | 100 | 15 | John Day Formation |
| 35-JE-289 | 46 - 1 | A | 72.76 | 14.37 | 2.40 | 0.46 | 5.16 | 2.65 | 0.42 | 1.61 | 0.17 | 100 | 18 | Mazama |
| 35-JE-296 | 411 - 1 | A | 72.74 | 14.40 | 2.42 | 0.45 | 5.09 | 2.61 | 0.03 | 1.64 | 0.20 | 100 | 15 | Mazama |
| 35-JE-298 | 301 - 3 | A | 72.86 | 14.40 | 2.42 | 0.41 | 5.00 | 2.67 | 0.46 | 1.60 | 0.17 | 100 | 17 | Mazama |
| 35-SH-134 | 15 - 1 | A | 72.78 | 14.33 | 2.44 | 0.42 | 5.09 | 2.69 | 0.46 | 1.61 | 0.18 | 100 | 21 | Mazama |
| 35-SH-134 | 20 - 1 | A | 72.82 | 14.36 | 2.46 | 0.41 | 5.01 | 2.69 | 0.47 | 1.61 | 0.17 | 100 | 17 | Mazama |
| 35-SH-134 | 22 - 2 | A | 72.84 | 14.30 | 2.48 | 0.41 | 5.11 | 2.65 | 0.45 | 1.58 | 0.18 | 100 | 18 | Mazama |
| 35-UM-154 | 323 - 1 | A | 73.06 | 14.30 | 2.36 | 0.41 | 5.00 | 2.69 | 0.44 | 1.56 | 0.18 | 100 | 21 | Mazama |
| 35-UM-154 | 323 - 1 | B | 77.06 | 12.94 | 1.32 | 0.16 | 3.96 | 2.82 | 0.23 | 1.32 | 0.19 | 100 | 4 | Glacier Peak |
| 35-UM-154 | 324 - 1 | A | 72.96 | 14.41 | 2.33 | 0.39 | 4.99 | 2.72 | 0.44 | 1.58 | 0.18 | 100 | 23 | Mazama |
| 35-UM-154 | 324 - 1 | B | 77.13 | 12.53 | 1.32 | 0.24 | 3.73 | 3.68 | 0.21 | 1.03 | 0.13 | 100 | 2 | Glacier Peak |
| 35-UM-154 | 326 - 1 | A | 73.01 | 14.34 | 2.32 | 0.42 | 4.98 | 2.72 | 0.46 | 1.57 | 0.18 | 100 | 23 | Mazama |
| 35-UM-154 | 326 - 1 | B | 76.83 | 12.90 | 1.50 | 0.21 | 4.00 | 3.51 | 0.20 | 0.75 | 0.10 | 100 | 1 | Unknown |
| 35-WS-120 | 395 - 1 | C | 72.87 | 14.42 | 2.44 | 0.42 | 4.98 | 2.66 | 0.45 | 1.59 | 0.18 | 100 | 15 | Mazama |
| 35-WS-120 | 412 - 1 | A | 72.88 | 14.44 | 2.41 | 0.43 | 4.95 | 2.65 | 0.46 | 1.61 | 0.18 | 100 | 16 | Mazama |
| 35-WS-120 | 444 - 1 | A | 75.47 | 13.44 | 1.88 | 0.23 | 4.32 | 3.26 | 0.21 | 1.08 | 0.12 | 100 | 13 | Unknown |
| 35-WS-120 | 444 - 1 | B | 76.63 | 13.43 | 1.41 | 0.16 | 4.07 | 2.34 | 0.30 | 1.54 | 0.11 | 100 | 11 | Mount St. Helens |
| 35-WS-120 | 444 - 1 | C | 76.04 | 13.05 | 1.68 | 0.18 | 4.30 | 3.72 | 0.16 | 0.74 | 0.14 | 100 | 9 | Unknown |

Major element results are reported in weight percent oxide; results are an average value of multiple analyses (see N= for the number of tephra shards analyzed).

[a] Geochemically distinguishable group(s) identified in an individual sample, e.g., A = geochemical group 1; B = geochemical group 2.

Table 7-3 (continued)

| Site | Specimen | Ash [a] | Chemical Composition | | | | | | | | | | | Tephra Source |
|---|---|---|---|---|---|---|---|---|---|---|---|---|---|---|
| | | | $SiO_2$ | $Al_2O_3$ | $Fe_2O_3$ | $TiO_2$ | $Na_2O$ | $K_2O$ | MgO | CaO | Cl | Total | N= | |
| 35-WS-120 | 444 - 1 | D | 71.85 | 14.91 | 2.94 | 0.33 | 4.90 | 2.61 | 0.49 | 1.88 | 0.10 | 100 | 4 | Unknown |
| 35-WS-120 | 444 - 1 | E | 68.46 | 15.43 | 4.33 | 0.59 | 4.88 | 2.42 | 0.97 | 2.81 | 0.10 | 100 | 3 | Unknown |
| 35-WS-223 | 26 - 1 | A | 72.84 | 14.43 | 2.41 | 0.42 | 5.01 | 2.63 | 0.47 | 1.62 | 0.17 | 100 | 12 | Mazama |
| 35-WS-223 | 26 - 1 | B | 76.11 | 12.12 | 2.74 | 0.18 | 2.09 | 5.91 | 0.03 | 0.76 | 0.06 | 100 | 16 | John Day Formation |
| 35-WS-225 | 134 - 1 | A | 73.27 | 14.23 | 2.48 | 0.40 | 4.84 | 2.63 | 0.46 | 1.53 | 0.16 | 100 | 20 | Mazama |
| 35-WS-225 | 187 - 1 | A | 73.14 | 14.23 | 2.49 | 0.40 | 4.93 | 2.60 | 0.47 | 1.55 | 0.18 | 100 | 22 | Mazama |
| 35-WS-225 | 217 - 1 | A | 73.36 | 14.12 | 2.46 | 0.39 | 4.93 | 2.59 | 0.46 | 1.50 | 0.17 | 100 | 18 | Mazama |
| 35-WS-225 | 258 - 1 | A | 72.94 | 14.35 | 2.43 | 0.39 | 5.03 | 2.67 | 0.46 | 1.57 | 0.16 | 100 | 20 | Mazama |
| 35-WS-226 | 100 - 1 | A | 72.91 | 14.39 | 2.45 | 0.43 | 4.98 | 2.65 | 0.45 | 1.59 | 0.15 | 100 | 18 | Mazama |
| 35-WS-230 | 218 - 1 | A | 72.89 | 14.34 | 2.44 | 0.41 | 5.05 | 2.65 | 0.02 | 1.58 | 0.19 | 100 | 17 | Mazama |
| 35-WS-231 | 421 - 1 | A | 73.03 | 14.39 | 2.25 | 0.44 | 4.99 | 2.67 | 0.44 | 1.59 | 0.18 | 100 | 17 | Mazama |
| 35-WS-231 | 424 - 1 | A | 72.90 | 14.39 | 2.38 | 0.42 | 5.01 | 2.66 | 0.46 | 1.61 | 0.16 | 100 | 20 | Mazama |
| 35-WS-231 | 427 - 1 | A | 72.85 | 14.39 | 2.46 | 0.40 | 5.03 | 2.59 | 0.45 | 1.61 | 0.21 | 100 | 15 | Mazama |
| 35-WS-232 | 46 - 1 | A | 72.76 | 14.36 | 2.47 | 0.42 | 5.06 | 2.69 | 0.46 | 1.60 | 0.18 | 100 | 18 | Mazama |
| 45-WW-100 | 207 - 1 | A | 77.42 | 12.59 | 1.32 | 0.20 | 3.75 | 2.99 | 0.26 | 1.30 | 0.17 | 100 | 18 | Glacier Peak |
| 45-WW-100 | 213 - 1 | A | 72.75 | 14.26 | 2.47 | 0.42 | 5.16 | 2.70 | 0.45 | 1.61 | 0.18 | 100 | 20 | Mazama |
| 45-WW-101 | 2 - 1 | A | 72.98 | 14.44 | 2.32 | 0.42 | 4.98 | 2.64 | 0.44 | 1.61 | 0.17 | 100 | 16 | Mazama |

Major element results are reported in weight percent oxide; results are an average value of multiple analyses (see N= for the number of tephra shards analyzed).

[a] Geochemically distinguishable group(s) identified in an individual sample, e.g., A = geochemical group 1; B = geochemical group 2.

### 7.3.2 Electron Microprobe Analysis

The electron microprobe employed in the characterization of the volcanic ash samples used an electron beam that is focused on the surface of a prepared sample. The beam is focused in an area ranging from 5 to 8 $\mu$m in diameter, permitting the analysis of individual volcanic ash glass shards. As an electron is knocked out of one shell by an impinging electron, it is replaced by another from an outer shell. The replacement results in the emission of an x-ray, the energy level of which is characteristic of each element. Based on the assumption that the intensity of a typical x-ray line generated per unit of time is directly proportional to the concentration of the target element, the peaks of the x-ray sample spectra can be quantified by comparing them with standards of known chemical composition (Johnson and Maxwell 1981). The compositions of samples reported in Table 7-3 are average values from multiple shards of analyzed tephra. The number of shards analyzed is also reported in this table.

Although the microprobe can be used to determine the abundances of elements with an atomic number greater than beryllium (Be), the relatively high detection limits and level of uncertainty for most trace elements generally limit analyses to the use of major and minor elements in the characterization of volcanic glass such as in tephras. While the major elements are not as sensitive in "fingerprinting" sources as the less abundant trace elements, they have proven useful and generally are reliable in the identification of sources of ash samples (Westgate and Briggs 1980).

### 7.3.3 Correlation of Samples with Characterized Geologic Sources

Primary source assignments were made by comparing the characterized archaeological tephra samples with previously analyzed primary sources of volcanic ash from the Western United States. Sources and samples were statistically correlated using a similarity coefficient (SC) (Borchardt et al. 1972). A resultant coefficient of 1.0 indicates a perfect match; a value of 0.95 to 0.99 generally indicates a correlation, while a coefficient of less than 0.88 indicates a high probability of error in matching archaeological samples and geologic sources. While a SC nearing 1.0 does not guarantee a perfect match between a sample and a source identity, it does indicate a high level of geochemical similarity (Davis 1985).

## 7.4 RESULTS OF ELECTRON MICROPROBE ANALYSES

The results of all electron microprobe analyses associated with PEP tephra samples are presented in Tables 7-2 and 7-3.

Multiple geochemical groups of tephra shards were identified in many of the tephra samples that were submitted for characterization. The presence of volcanic ash from different sources is generally attributed to postdepositional transport and mixing of tephra from different eruptive events. Volcanic ash is easily eroded and reworked, and may be rapidly stripped from surfaces by sheetwash and aeolian processes. This is often reflected in the samples collected, which commonly contain individual tephra grains from more than one source but are dominated by glass from a single eruption. In some cases involving unknown sources, the identification of multiple groups is tentative; the two groups may represent only the geochemical variability of a single eruption.

The results of the electron microprobe analyses are summarized as scatterplots in Figures 7-3 and 7-4. In these plots, CaO is plotted versus $K_2O$ and $Fe_2O_3$ to allow visual discrimination among the different tephra sources. These three elements often maintain a minimal degree of intrasource chemical variability while showing considerable variability between different tephra sources. This characteristic often makes these three elements useful in the identification and correlation of geochemically discrete clusters of samples.

Two major clusters of samples stand out in the scatterplots. One of these consists of the numerous samples originating from the Mazama eruptions. Also apparent in the plots is the similarity among samples of John Day Formation tuff, and the relatively high-potassium ash that was recovered from several north-central Oregon archaeological sites. The possible origin of these high-potassium tephra are discussed in the following section.

## 7.5 DISCUSSION

### 7.5.1 Mazama Tephra

Tephra originating from the Mazama eruptions was identified in samples from 17 Oregon sites and one site each in California, Washington, and Idaho (Figure 7-1 and Table 7-1). All occurrences of Mazama ash were found within the mapped geographic limits of the airfall deposits from the climactic eruptions dated at 6,800 B.P. (Bacon 1983).

### 7.5.2 Glacier Peak Tephra

Tephra shards originating from Glacier Peak eruptions of about 11,200 B.P. were identified at a single Oregon site (35-UM-154) and one Washington site (45-WW-100). These results are generally consistent with the known geographic distribution of Glacier Peak tephra, although 35-UM-154 lies near the southern boundaries of ash fall recognized from Glacier Peak.

### 7.5.3 Mount St. Helens Tephra

Tephra deposited from eruptions of Mount St. Helens was identified at 35-WS-120 in north-central Oregon. The tephra collected at this site appears to have a similar composition to tephra units Jy, S, We, and Ye, which are associated with eruptions that span the period from the very late Pleistocene (layer S) to the early Holocene (layer We) (Mullineaux 1986).

### 7.5.4 Glass Mountain Tephra

A single ash sample collected from CA-MOD-2561 is correlated with tephra from the Medicine Lake Highlands based on geochemical similarities. This site falls within the boundaries of Glass Mountain ash fall, and it is almost certain that the ash originated during the Glass Mountain eruption of about 850–900 B.P. (Donnelly-Nolan et al. 1990; Heiken 1978).

### 7.5.5 High-Potassium John Day Region Glasses

Of particular interest is a group of samples of high-potassium glasses (4.5–9.0% $K_2O$) that was identified at several sites in north-central Oregon (see Figure 7-1 and Table 7-1). The ash co-occurs with deposits of tephra from other sources and is found as a significant, though not dominant, component of the total characterized ash shards identified from any one

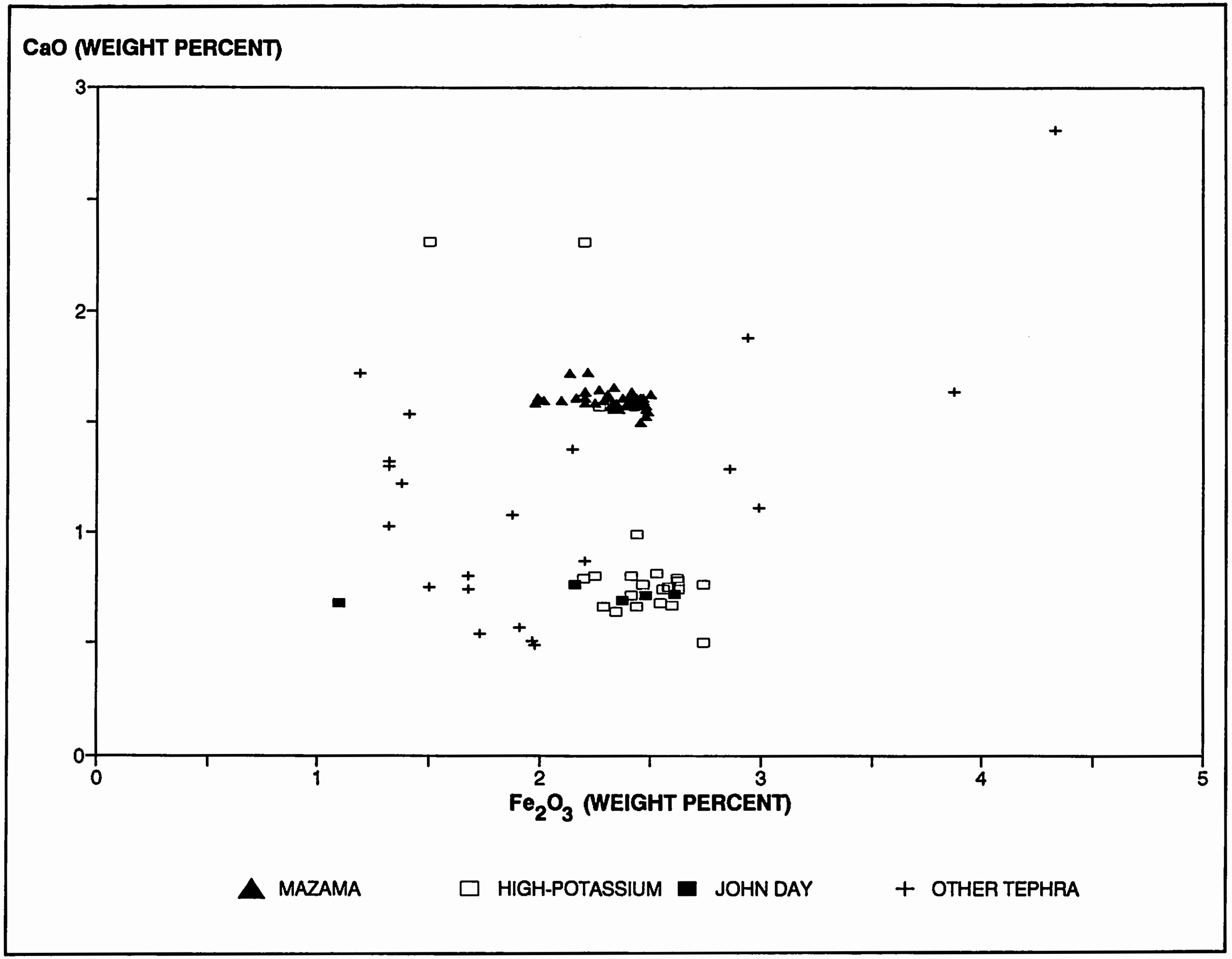


Figure 7-3 Scatterplot of CaO plotted versus $K_2O$ for PEP tephra samples.

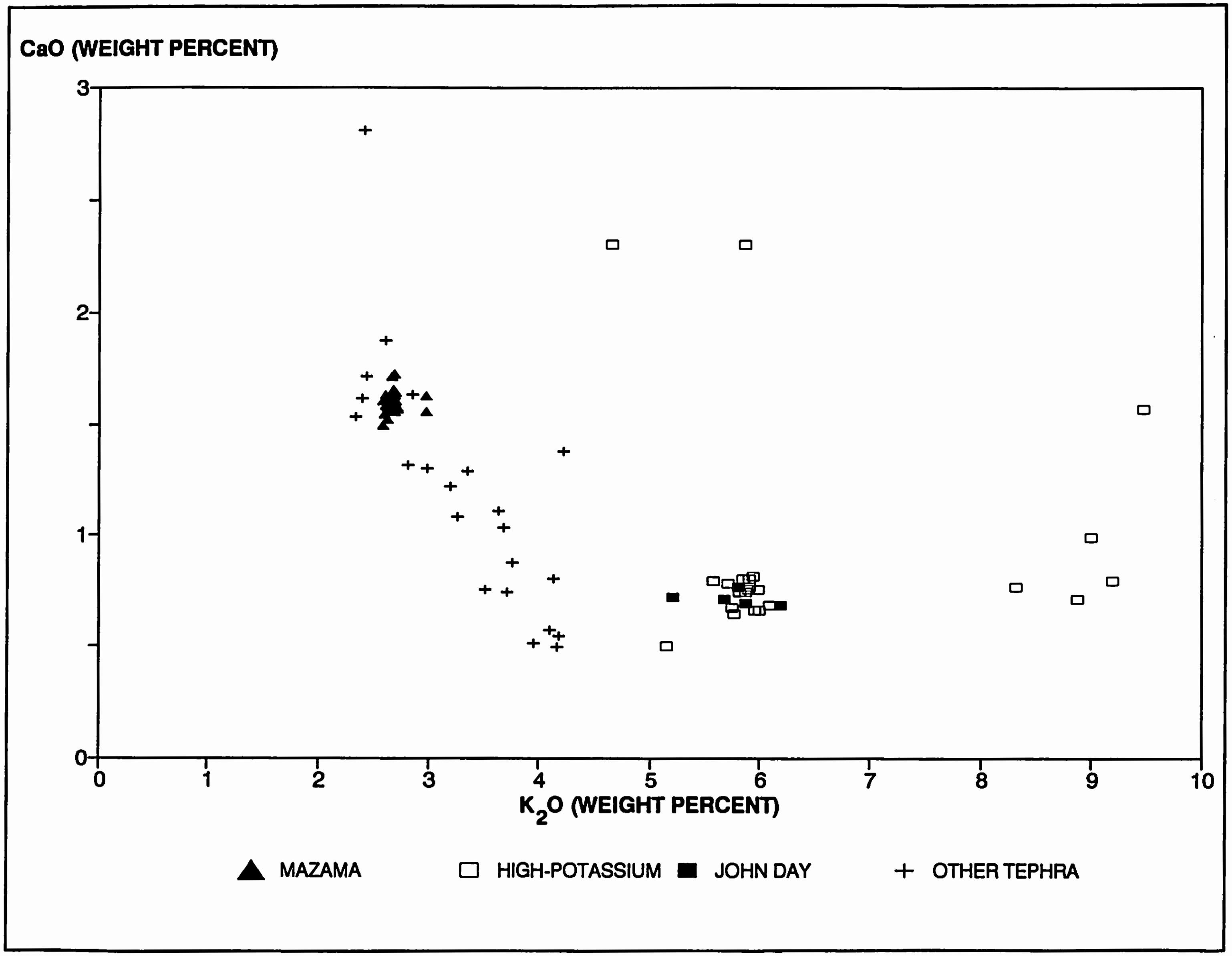


Figure 7-4 Scatterplot of CaO plotted versus $Fe_2O_3$ for PEP tephra samples.

sample. The distribution of the high-potassium tephras was also found to coincide with the bedrock occurrence of the John Day Formation tuffs. The Oligocene-age John Day Formation consists largely of ignimbrites and airfall sheets (Robinson et al. 1984, 1990) that are readily weathered and eroded when exposed in outcrop. It appears that secondary deposition by alluvial and aeolian processes may be contributing glass shards from outcrop areas of the John Day Formation to primary tephra deposits originating from more recent Holocene eruptions. A tuff sample collected from bedrock exposures at 35-JE-51B (2392-1) was found to contain as many as five compositionally distinct groups of tephra. The major element composition of the high-potassium groups is similar to those from the John Day tuffs which outcrop at the site, and it appears that at least 18 of the analyzed high-potassium glasses originated from the bedrock tuff source (Figure 7-1) (Franklin F. Foit, personal communication, 1992). Compositional analyses of samples collected from the John Day Formation bedrock and from tephra samples from selected archaeological site contexts are graphically shown in Figures 7-3 and 7-4. The composition of glass from these two sample groups plot in nearly the same field area, and are comparable to analyses reported from the John Day Formation by Robinson et al. (1984, 1990). The other analyzed samples of glasses with $K_2O$ exceeding 8 percent remain unassigned to a specific source at the present time, although it is likely that their origin is from a local ash-flow tuff outcrop.

### 7.5.6 Pleistocene Tephra Sources

Several geochemical groups of ash shards were tentatively correlated with Pleistocene tephra beds found at Summer Lake (Oregon), Wono Lake Beds (California), Trego Hot Springs (California), and Clear Lake Beds (California). These deposits are described by Davis (1985) and Sarna-Wojcicki et al. (1987, 1988, and 1991).

Similarity coefficient (SC) values from two chemically distinguishable groups of ash collected at 35-JE-283 (Sample 916-1; Ashes A and C) were high when compared to tephra from several Pleistocene sources—Summer Lake Beds O and S and the Wono Lake Tephra Bed.

One of two groups of glasses identified in pre-occupation levels at 35-DS-557 yielded high SC values of 0.97 when compared, respectively, to tephra found at Summer Lake, Oregon (>117,000 B.P.), and Clear Lake, California (55,000–75,000 B.P.). The SC values of 0.95–0.96 resulted when the second group of glass was compared with somewhat younger beds at Summer Lake, Oregon.

One of the shards analyzed from 35-UM-154 (Sample 326-1; Ash B) showed a glass chemistry similar to the Trego Hot Springs Bed, although the very low sample size (n=1) and SC of 0.93 suggests only a very tentative correlation.

The similarity of Ash B from CA-MOD-2573 (Sample 204-1) with the Olema ash bed is suggested by Andrei Sarna-Wojcicki (personal communication, 1991). The age of this bed, based on correlations and age estimates of ash beds in Quaternary sediments at Clear Lake, California, is estimated at between 55,000 and 75,000 B.P. (Sarna-Wojcicki et al. 1988).

### 7.5.7 Unknown Tephra Sources

Sources remain unidentified for 23 of the geochemical groups of glass shards that were analyzed, as discussed earlier. Some of this material probably originated from redeposition of older ash-flow tuffs of the John Day Formation. Others may represent undocumented variability in compositional ranges from known primary sources or as yet undefined, new primary sources. In addition, the shards that makes up the tephra samples may be affected by diagenetic alteration of the glass and by the selective leaching of trace elements, resulting in chemical fingerprints that become less distinct over time (Fisher and Schmincke 1984).

## 7.6 CONCLUSIONS

Volcanic tephra originating from the ca. 6,800 B.P. eruptions of Mount Mazama was identified in samples collected at 21 sites in Washington, Oregon, and northern California, and was the most readily identifiable tephra encountered in an archaeological context within the Project area. Other Holocene tephras identified during the Project include: Glacier Peak (ca. 11,200 B.P.), found at a site in southeast Washington and a site in northern Oregon; Glass Mountain (850-900 B.P.), found at sites on the Modoc Plateau east of the Medicine Lake Highlands; and ash from a possible unidentified Mount St. Helens set, identified from a single north-central Oregon site, 35-WS-120. In addition, tephra from older Pleistocene tephra sources was tentatively identified at several sites. These older ash deposits were probably reworked from pre-occupation sediments adjacent to sites or were introduced as a minor component into more recent tephra through postdepositional mixing.

High-potassium glasses from sources that were tentatively unidentified at several north-central Oregon sites during testing and early data recovery phases of the Project have been correlated with ash-flow tuffs associated with the John Day Formation. The occurrence of these glass shards admixed with younger tephra and more recent archaeological deposits is the result of mixing and intrusion by natural site-formation processes from nearby bedrock exposures. Several of the other high-potassium glasses analyzed may have originated from other local bedrock units, and their source remains unassigned at the present time.

In summary, tephrochronologic investigations help define significant time-correlative geologic markers that are used to understand site formation processes and develop chronological sequences at numerous archaeological sites. Tephra studies often provided, in conjunction with obsidian hydration measurements, the only chronological data at archaeological sites where carbon-dating methods were not practicable.

# Attachment 7-1

**Letter Reports by Dr. Franklin F. Foit, Department of Geology, Washington State University, Describing Results of 1992–1993 PEP Volcanic Tephra Electron Microprobe Analyses**

Washington State University

Department of Geology

Pullman, WA 99164-2812
509-335-3009
FAX: 509-335-7816

September 22, 1992

Mr. Craig E. Skinner
Assistant Laboratory Director
Infotec Research Inc.
78 Centennial Loop, Suite H
Eugene, OR 97401

Craig,

We have run the nine samples you sent. Sorry for the delay in getting the results to you but your samples arrived just as two of my techs were leaving on a long vacation.

All of the 35-JE-49 samples (1462-2, 1464-2, 1467-2, 1469-2) and appear to contain only Mazama glass (Table 1). The ten best matches from our databank search were all Mazama tephras with similarity coefficients ranging from 0.97 to 0.99. Samples 35-JE-283-398-2, 35-JE-283-439-2 and 35-JE-51B-2763-2 also contain a significant proportion of what appears to be Mazama glass from the 6850 BP eruption along with a higher Si and K glass which I have called glass B. Glass B has been observed in many samples, we have previously analyzed for you, especially in those from around Willowdale, OR. The source of this glass remains a mystery.

In addition to Glass B, sample 35-JE-283-916-1 contains minor amounts of a Glass A and major amounts of Glass C. Glass A is similar in chemistry to Summer Lake Tephra Beds O (SC = 0.95), P (SC=0.94) and Wono Lake Tephra Bed (24,800 BP)(SC=0.94). Glass C compares reasonably well (SC = 0.93) to Summer Lake Tephra Bed S, Summer Lake, OR. These beds are described in Davis (1985) (Quat. Res. 23, 38-53).

In addition to Glass B, sample 35JE51B contains major amounts of Glass D and minor amounts of Glass E. Glass D is a poor match (SC = 0.87, Na is way off) to Glass B in sample 35JE51B, TR-201 from near Willowdale, OR and Glass E doesn't reliably match anything in our databank. Just to put these similarity coefficients (SC) in perspective, a value of 1.0 is a perfect match and there is a high probability of error in matches with SCs less than 0.88.

I hope this data is of value to you and if you have any questions please give me a call.

Sincerely,

Franklin F. Foit, Jr.
Director of Microbeam Lab

## TABLE 1. GLASS CHEMISTRY OF INFOTEC RESEARCH TEPHRAS

| Oxide | 35-JE-49 | 35-JE-49 | 35-JE-49 | 35-JE-49 | 35-JE-283 | | 35-JE-283 | |
|---|---|---|---|---|---|---|---|---|
| | 1464-2 | 1462-2 | 1467-2 | 1469-2 | 439-2 | | 398-2 | |
| | Mazama | Mazama | Mazama | Mazama | Mazama | Glass B | Mazama | Glass B |
| SiO2 | 73.12(36) | 73.20(17) | 73.28(34) | 73.34(39) | 73.14(24) | 76.31(21) | 73.09(25) | 76.25(27) |
| Al2O3 | 14.47(14) | 14.52(13) | 14.46(12) | 14.48(15) | 14.48(24) | 12.25(11) | 14.48(15) | 12.23(9) |
| Fe2O3 | 2.00(12) | 2.02(10) | 1.98(8) | 1.99(11) | 2.21(15) | 2.29(11) | 2.17(15) | 2.44(16) |
| TiO2 | 0.47(12) | 0.41(3) | 0.41(2) | 0.43(9) | 0.45(3) | 0.18(4) | 0.41(4) | 0.21(9) |
| Na2O | 5.05(17) | 4.96(11) | 4.94(15) | 4.81(26) | 4.94(21) | 2.16(27) | 2.17(15) | 2.12(6) |
| K2O | 2.66(6) | 2.66(7) | 2.67(7) | 2.69(9) | 2.61(8) | 6.00(16) | 4.94(18) | 5.95(19) |
| MgO | 0.46(3) | 0.46(4) | 0.45(3) | 0.46(3) | 0.45(3) | 0.02(2) | 0.45(4) | 0.02(1) |
| CaO | 1.60(13) | 1.60(6) | 1.59(6) | 1.61(7) | 1.59(9) | 0.66(10) | 1.61(8) | 0.66(11) |
| Cl | 0.17(4) | 0.17(1) | 0.21(6) | 0.19(10) | 0.16(4) | 0.13(7) | 0.16(4) | 0.12(3) |
| Total | 100 | 100 | 100 | 100 | 100 | 100 | 100 | 100 |
| | n=16 | n=15 | n=13 | n=17 | n=17 | n=12 | n=16 | n=12 |

Key Atom Percentages

| | | | | | | | | |
|---|---|---|---|---|---|---|---|---|
| Ca | 24.1(1.9) | 24.0(0.9) | 24.0(0.9) | 24.1(1.0) | 23.4(1.3) | 6.7(1.0) | 23.5(1.2) | 6.6(1.1) |
| K | 46.5(1.8) | 46.4(1.2) | 46.8(1.2) | 46.8(1.6) | 44.7(1.4) | 70.6(1.9) | 45.6(1.9) | 69.4(2.2) |
| Fe | 29.4(1.8) | 29.6(1.5) | 29.2(1.2) | 29.1(1.6) | 31.9(2.2) | 22.7(1.1) | 30.9(2.1) | 24.0(1.6) |
| K/Fe | 1.58(0.10) | 1.56(0.09) | 1.60(0.08) | 1.61(0.10) | 1.40(0.10) | 3.11(0.17) | 1.47(0.12) | 2.90(0.21) |

* standard deviations in parentheses
n = number of point analyses averaged

**Table 1. Con't**

| Oxide | 35-JE-283 916-1 Glass A | Glass B | Glass C | 35-JE-51B 2763-2 Mazama | Glass B | 35-JE-51B 2350-2 Glass B | Glass D | Glass E |
|---|---|---|---|---|---|---|---|---|
| $SiO_2$ | 72.37(1) | 76.24(48) | 73.84(34) | 73.05(48) | 76.39(29) | 76.29(34) | 75.31(42) | 77.10(1.02) |
| $Al_2O_3$ | 14.54(3) | 12.20(13) | 14.06(22) | 14.47(17) | 12.30(12) | 12.28(14) | 12.15(19) | 12.53(29) |
| $Fe_2O_3$ | 2.86(6) | 2.35(10) | 2.21(15) | 2.10(11) | 2.20(20) | 2.25(33) | 2.20(17) | 1.50(18) |
| $TiO_2$ | 0.30(3) | 0.18(4) | 0.20(3) | 0.44(4) | 0.17(3) | 0.21(6) | 0.17(3) | 0.19(2) |
| $Na_2O$ | 4.85(8) | 2.45(41) | 4.83(14) | 5.05(24) | 2.27(22) | 2.22(24) | 0.10(10) | 1.43(32) |
| $K_2O$ | 3.35(8) | 5.77(20) | 3.76(12) | 2.66(11) | 5.80(19) | 5.85(16) | 9.20(52) | 4.66(38) |
| MgO | 0.32(3) | 0.02(2) | 0.14(3) | 0.44(2) | 0.02(3) | 0.04(4) | 0.03(4) | 0.26(15) |
| CaO | 1.29(11) | 0.64(1) | 0.87(10) | 1.60(7) | 0.76(10) | 0.80(16) | 0.79(7) | 2.31(28) |
| Cl | 0.12(4) | 0.15(1) | 0.09(6) | 0.19(3) | 0.08(4) | 0.08(6) | 0.05(4) | 0.02(3) |
| Total | 100 | 100 | 100 | 100 | 100 | 100 | 100 | 100 |
| | n=2 | n=13 | n=10 | n=9 | n=14 | n=10 | n=9 | n=3 |

Key Atom Percentages

| | | | | | | | | |
|---|---|---|---|---|---|---|---|---|
| Ca | 16.2(1.4) | 6.6(1.0) | 11.8(1.4) | 23.7(1.0) | 7.9(1.0) | 8.2(1.6) | 5.8(0.7) | 25.1(3.0) |
| K | 48.8(1.2) | 69.5(2.4) | 59.0(1.9) | 45.8(1.9) | 69.8(1.3) | 69.3(1.9) | 78.4(1.4) | 58.9(6.6) |
| Fe | 35.0(0.7) | 23.8(1.0) | 29.2(2.0) | 30.5(1.6) | 22.3(2.0) | 22.5(3.3) | 15.8(1.2) | 16.0(1.9) |
| K/Fe | 1.39(0.04) | 2.91(0.16) | 2.02(0.15) | 1.50(0.10) | 3.13(0.29) | 3.09(0.46) | 4.97(0.39) | 3.69(0.60) |

* standard deviations in parentheses
n = number of point analyses averaged

Washington State University
Department of Geology
Pullman, WA 99164-2812
509-335-3009
FAX: 509-335-7816

October 30, 1992

Mr. Craig E. Skinner
Assistant Laboratory Director
Infotec Research Inc.
78 Centennial Loop, Suite H
Eugene, OR 97401

Craig,

We ran the sample of the John Day Formation from near site 35-JE-51B and the results are quite interesting and fruitful. The glasses (massive brown and a stringy colorless pumice) found in the sample were is remarkably good shape so our analytical problems were few. As I recall many of the Willowdale samples contained a massive brown glass. I believe there are two or perhaps three glasses represented in this sample but to be sure were searched every likely chemical grouping and subgrouping and I've enclosed the search output.

The first entry in Table 1 is the chemistry of all the glass shards analyzed. Note that the bulk composition is a reasonably good match for many of the glasses found in in previous samples from the Willowdale area. There may be more but the new algorithm for my search routine only prints out the closest 15 matches. This strongly suggests that much of the tephra we've analyzed is redeposited material from the John Day Formation. In an effort to refine the search I then ran the chemistry of the two morphologically distinct glasses (massive brown and stringy pumice). Most of the matches for the massive brown glass component are the same as for the bulk glass chemistry, only the ordering is different. The stringy pumice shows generally poor matches with Infotec samples but a fair match with Ash Bed 5 from Clear Lake, CA. I then broke the massive brown shards into two chemical groups (which also matched their depth of color pretty well). The dark brown and particularly the light fraction has many matches in common with the massive brown group. In addition in the massive dark brown group there are poor matches (especially for the key elements Fe, Ca and K) to Huckleberry Ridge glasses.

Because we had to do quite a bit more preparation and analysis of this sample I've had to charge a bit more ($275). If this presents a problem or you want to chat about the results, give me a call. Happy Halloween.

Good Luck,

Nick

TABLE 1. GLASS CHEMISTRY OF INFOTEC RESEARCH ASH FLOW TUFF IN JOHN DAY FORMATION

| Oxide | 35-JE-51B bulk composition | 35-JE-51B massive brown glass | 35-JE-51B stringy pumice | 35-JE-51B massive light brown | 35-JE-51B massive dark brown |
|---|---|---|---|---|---|
| SiO2 | 76.40(82) | 76.08(66) | 77.41(23) | 76.38(45) | 75.78(23) |
| Al2O3 | 12.20(29) | 12.14(29) | 12.40(16) | 12.13(18) | 11.98(13) |
| Fe2O3 | 2.16(68) | 2.48(37) | 1.10(17) | 2.38(35) | 2.61(16) |
| TiO2 | 0.19(5) | 0.19(6) | 0.17(4) | 0.19(5) | 0.19(4) |
| Na2O | 2.45(54) | 2.60(53) | 1.94(9) | 2.28(19) | 3.36(25) |
| K2O | 5.79(41) | 5.68(39) | 6.19(11) | 5.87(19) | 5.21(39) |
| MgO | 0.04(4) | 0.03(3) | 0.07(5) | 0.03(2) | 0.02(2) |
| CaO | 0.71(12) | 0.71(12) | 0.68(13) | 0.69(11) | 0.72(11) |
| Cl | 0.06(5) | 0.07(5) | 0.04(1) | 0.05(4) | 0.13(2) |
| Total | 100 | 100 | 100 | 100 | 100 |
| | n=39 | n=28 | n=9 | n=20 | n=8 |

Key Atom Percentages

| | | | | | |
|---|---|---|---|---|---|
| Ca | 7.4(1.3) | 7.3(1.2) | 7.6(1.5) | 7.0(1.1) | 7.7(1.2) |
| K | 70.5(5.0) | 67.8(4.7) | 80.4(1.4) | 69.3(2.2) | 64.9(4.9) |
| Fe | 22.1(6.9) | 24.9(3.7) | 12.0(1.9) | 23.7(3.5) | 27.4(1.7) |
| K/Fe | 3.2(1.0) | 2.7(0.4) | 6.7(1.0) | 2.9(0.4) | 2.4(0.2) |

* standard deviations in parentheses
n = number of point analyses averaged

Washington State University

Department of Geology

Pullman, WA 99164-2812
509-335-3009
FAX: 509-335-7816

April 16, 1993

Mr. Craig E. Skinner
Assistant Laboratory Director
Infotec Research Inc.
78 Centennial Loop, Suite H
Eugene, OR 97401

Craig,

I finally got around to running the sample you sent me about a month ago. Unfortunately, your sample arrived one day after we ran a large batch so I had to wait until we accumulated another group of samples.

The sample you sent consisted of ~90% diatoms, ~ 2-3% mineral matter and ~7-8% glass. Most of the glass (glass 1, Table) had tight chemistry but there were also a few shards of quite variable chemistry. Only two of these additional shards had a similar chemistry (glass 2, Table). To my surprise a search of our data bank yielded some pretty good matches (similarity coefficient = 0.97) for an older tephra (>117,000 B.P.) found at Summer Lake, OR and younger ones (55,000-75,00 B.P.) at Clear Lake, CA. Likewise the average chemistry of the other two shards matches (SC = 0.95-0.96) those of slightly younger beds at Summer Lake. I've enclosed the output from our search routine which details the similarity coefficients and gives you references to the work at Summer and Clear Lakes. If you have any questions give me a buzz.

Good Luck,

Nick

**TABLE 1. GLASS CHEMISTRY OF INFOTEC "ASH" SAMPLE**

| Oxide | 35-DS-557-2276-1 Glass 1 | Glass 2 |
|---|---|---|
| SiO2 | 75.25(28) | 69.99 |
| Al2O3 | 13.24(12) | 14.83 |
| Fe2O3 | 1.73(12) | 3.88 |
| TiO2 | 0.17(4) | 0.53 |
| Na2O | 4.63(23) | 5.63 |
| K2O | 4.19(18) | 2.85 |
| MgO | 0.10(1) | 0.53 |
| CaO | 0.54(5) | 1.64 |
| Cl | 0.15(2) | 0.1 |
| Total | 100 | 100 |
| | n=20 | n=2 |

Key Atom Percentages

| | | |
|---|---|---|
| Ca | 7.6(0.7) | 18.8 |
| K | 68.6(2.9) | 43.4 |
| Fe | 23.8(1.7) | 37.8 |
| K/Fe | 2.88(0.23) | 0.87 |

* standard deviations in parentheses
n = number of point analyses averaged

Washington State University
Department of Geology
Pullman, WA 99164-2812
509-335-3009
FAX: 509-335-7816

April 16, 1993

Mr. Craig E. Skinner
Assistant Laboratory Director
Infotec Research Inc.
78 Centennial Loop, Suite H
Eugene, OR 97401

Dear Craig,

Here are the results on the three samples you provided from Oregon archaeological site 35-UM-154. All of the tephra in these samples appears to be re-deposited as evidenced by the high sediment content, rounding of the grains and the likely presence of tephra from more than one source. As you can see from the data in Table 1 the bulk composition of the glass in each sample is quite similar to (but with high standard deviations) and keys out as Mazama with high similarity coefficients (similarity coefficient = 0.98). However, in each of the samples there appears to be a small amount of glass from other sources and when this data is segregated from the Mazama data (glass 1 in all samples) the standard errors are appreciably lowered and the matches for Mazama become even better (SCs = 0.99). In samples 323-1 and 324-1 the other glass appears to be from Glacier Peak. Glacier Peak tephra has been found at other sites in this area. The "other" glass (es) in Sample 326-1 has an extremely variable chemistry and doesn't "group" well. One of the shards analyzed (although this isn't much to go on) has a chemistry similar (SC = 0.93) to glass from the Trego Hot Springs.

If you have any questions give me a call.

Sincerely,

Nick

Franklin F. Foit, Jr.
Professor and Chair
Director Microbeam Lab

**TABLE 1. GLASS CHEMISTRY OF INFOTEC SAMPLES FROM SITE 35-UM-154**

| Oxide | 35-UM-154-323-1 | | | 35-UM-154-324-1 | | | 35-UM-154-326-1 | | |
|---|---|---|---|---|---|---|---|---|---|
| | Bulk Composition | Glass 1 | Glass 2 | Bulk Composition | Glass 1 | Glass 2 | Bulk Composition | Glass 1 | Glass 2 |
| SiO2 | 73.15(1.33) | 73.06(20) | 77.06(25) | 73.24(1.25) | 72.96(19) | 77.13(4) | 73.15(1.33) | 73.01(25) | 76.83 |
| Al2O3 | 14.26(42) | 14.30(15) | 12.94(48) | 14.29(60) | 14.41(13) | 12.53(14) | 14.26(42) | 14.34(8) | 12.90 |
| Fe2O3 | 2.40(67) | 2.36(11) | 1.32(23) | 2.23(32) | 2.33(13) | 1.32(3) | 2.40(67) | 2.32(18) | 1.50 |
| TiO2 | 0.42(14) | 0.41(4) | 0.16(9) | 0.38(7) | 0.39(5) | 0.24(3) | 0.42(14) | 0.42(3) | 0.21 |
| Na2O | 4.65(86) | 5.00(9) | 3.96(25) | 4.91(33) | 4.99(19) | 3.73(9) | 4.65(86) | 4.98(9) | 4.00 |
| K2O | 2.93(67) | 2.69(7) | 2.82(48) | 2.79(32) | 2.72(7) | 3.68(55) | 2.93(67) | 2.72(5) | 3.51 |
| MgO | 0.45(11) | 0.44(4) | 0.23(3) | 0.42(8) | 0.44(4) | 0.21(5) | 0.45(11) | 0.46(3) | 0.20 |
| CaO | 1.55(30) | 1.56(8) | 1.32(11) | 1.56(21) | 1.58(6) | 1.03(26) | 1.55(30) | 1.57(7) | 0.75 |
| Cl | 0.19(13) | 0.18(3) | 0.19(10) | 0.18(3) | 0.18(3) | 0.13(4) | 0.19(13) | 0.18(3) | 0.10 |
| Total | 100 | 100 | 100 | 100 | 100 | 100 | 100 | 100 | 100 |
| | n=25 | n=21 | n=4 | n=23 | n=20 | n=2 | n=23 | n=17 | n=1 |
| **Key Atom Percentages** | | | | | | | | | |
| Ca | 22.4(2.9) | 22.3(1.1) | 22.5(1.9) | 22.4(1.6) | 22.5(0.9) | 15.6(3.9) | 21.2(4.1) | 22.4(1.0) | 11.9 |
| K | 46.1(4.2) | 44.7(1.2) | 55.6(9.5) | 46.4(5.3) | 45.0(1.2) | 64.8(9.7) | 46.6(10.7) | 45.2(0.8) | 64.7 |
| Fe | 31.5(6.6) | 33.0(1.5 | 21.9(3.8) | 31.2(4.5) | 32.5(1.8) | 19.6(0.4) | 32.2(9.0) | 32.4(2.5) | 23.3 |
| K/Fe | 1.46(0.23) | 1.35(0.07) | 2.54(0.62) | 1.49(0.18) | 1.39(0.06) | 3.31(0.15) | 1.45(0.52) | 1.39(0.11) | 2.78 |
| Source | Mazama | Mazama | Glacier Peak | Mazama | Mazama | Glacier Peak | Mazama | Mazama | Trego Hot Springs |
| Age | 6850 BP | 6850 BP | 11,200 BP | 6850 BP | 6850 BP | 11,200 BP | 6850 BP | 6850 BP | 23,400 BP |
| Sim. Coeff. | 0.98 | 0.99 | 0.96 | 0.98 | 0.99 | 0.93-0.94 | 0.98 | 0.99 | 0.93 |

* standard deviations in parentheses
n = number of point analyses averaged